arXiv:1302.1827v1 [physics.atom-ph] 7 Feb 2013

Vibrational spectroscopy of polar molecules with superradiance

Guin-Dar Lin and Susanne F. Yelin
ITAMP, Harvard-Smithsonian Center for Astrophysics and Harvard Physics Department, Cambridge, Massachusetts 02138, USA and
Department of Physics, University of Connecticut, Storrs, Connecticut 06269, USA

We investigate cooperative phenomena and superradiance for vibrational transitions in polar molecule spectroscopy when a high optical-depth (OD) sample is studied. Such cooperativity comes from the build-up of inter-particle coherence through dipole-dipole interactions and leads to the speed-up of decay process. We compare our calculation to recent work [Deiglmayr et al., Eur. Phys. J. D 65, 99 (2011)] and find very good agreement, suggesting that superradiant effects need to be included in a wide variety of ultracold molecule setups including vibrational and rotational states.

I. INTRODUCTION

Ultracold molecules have recently become an intensely explored area due to their fascinating properties. Many proposals have been brought up, for example, to improve the precision measurement of fundamental constants [1, 2], or test the fundamental law of physics, *e.g.*, [3]. As expected, the question of how to gain better access to internal degrees of a molecule to help better manipulation becomes an important step. The most commonly used tool of analysis in molecule systems is spectroscopy. However, for molecules the resolution of complicated spectral lines with necessary accuracy is crucial. Typically, the spectroscopic model for internal degrees of a molecule has also been applied to an ensemble, by assuming that the overall radiative behavior does not deviate dramatically from the direct sum of individual responses of the ingredient molecules. Even in the case of amplified spontaneous emission (ASE, also called "superluminescence") [4, 5], where the medium nonlinearity plays an important role, the inter-particle coherence in terms of genuine quantum manybody nature is usually overlooked. Such quantum manybody coherence can modify the emission rate significantly, resulting in "superradiance", which was first predicted by Dicke in 1954 [6]. Since then plenty of efforts have been made to investigate such phenomena both theoretically [5, 7–13] and experimentally [4, 14–20]. The interest in superradiance has been revived especially during recent years due to the advances of controlling atomic, molecular, and other quantum optical systems [21–23].

Looking at the simplest model, Dicke considered a case where the ensemble of excited two-level particles is confined in space to a size much smaller than the transition wavelength. In the limiting case where we are allowed to regard the whole ensemble as a point-like system, the system can be described by a collective spin $J = N/2$ with N the number of particles and the factor $\frac{1}{2}$ is for two-level atoms analogous to spin-$\frac{1}{2}$ particles. As a result the overall decay rate is now given by $\Gamma(J, M) = \gamma\langle JM|D^+D^-|JM\rangle$, where γ is the free-space spontaneous decay rate, the collective raising operator $D^+ = \sum_i |e\rangle_i\langle g|$ with particle index i and the lowering operator $D^- = (D^+)^\dagger$; M is the index of the Dicke ladder with $-J \leq M \leq J$. This factor $\langle JM|D^+D^-|JM\rangle = (J - M)(J + M - 1)$ quantifies the enhancement of the decay rate, contributing to the origin of superradiance [6, 13].

Note that in the above discussion for Dicke superradiance, the sample size is considered infinitesimally small compared to the transition wavelength λ. In reality, the particle ensemble must have a finite spread in space. Also, the distance-dependent dipole-dipole interaction breaks the Dicke symmetry and causes considerable dephasing. A quantity called cooperativity can be defined to characterize the competition of these two length scales: $\mathcal{C} \equiv \mathcal{N}\lambda^3/(4\pi)$, where $\mathcal{N}$ is the volume density of particles. As one can expect, superradiance is more obvious when $\mathcal{C} \gg 1$ but getting suppressed when $\mathcal{C}$ decreases. However, according to further analysis [7, 24–28], it is more accurate to characterize superradiance behavior by the optical depth $\mathrm{OD} \equiv \mathcal{N}\lambda^2 d$ with sample diameter d, consistent with the known fact that the superradiance can be directional and hence depends on the geometry of the sample. Recent experimental technology has allowed to realize high OD for atomic and molecular ensembles. Therefore, cooperative phenomena such as superradiance should be observable in such systems. Indeed, a study on rubidium Rydberg atoms dealing with Rydberg state relaxation has showed that the associated life time is considerably shortened given $\mathrm{OD} \approx 10^5$ [29, 30]. Its decay behavior agrees quite well with the theoretical calculation in our previous work [30], suggesting the emergence of superradiance.

In this paper, we want to discuss the same effects for polar molecules specially for vibrational spectroscopy for which the parameter regime is accessible by current technology. We have developed an effective two-body formalism that accounts for the actual dipole-dipole interaction for finite OD, for which the Dicke picture fails to be valid. We also compare our calculation to a recent experiment on the vibrational relaxation of LiCs molecules [31]. Even though in this experiment OD is rather small such that the superradiance feature is not dominant, we observe a discrepancy between the measured data and the results given by the traditional single-particle rate equation approach including blackbody radiation. Such disagreement is not found when superradiance physics is

	μ (u)	ω_e (cm^{-1})	$\wp$ (D)	OD ($\times 10^3$)
^{7}Li^{39}K	5.95	207	3.4	1.2
^{7}Li^{85}Rb	6.48	185	4.0	1.5
^{7}Li^{133}Cs	6.66	167	5.5 [31, 32]	1.8
^{23}Na^{39}K	14.5	124	2.8 [32]	3.3
^{23}Na^{85}Rb	18.1	107	3.1	4.4
^{23}Na^{133}Cs	19.6	98	4.7	5.2
^{39}K^{85}Rb	26.7	76	0.57 [33]	8.7
^{39}K^{133}Cs	30.1	66	1.9 [32]	12
^{85}Rb^{133}Cs	51.8	49	1.3 [32]	21
Rb (Rydberg)		33	$\sim 10^3$	83

Table I: Table of the reduced masses μ, vibrational spacing ω_e, dipole moments $\wp$, and optical depths OD, for various alkali diatomic molecules. To estimate OD , we assume $\mathcal{N} = 5 \times 10^9 \mathrm{cm}^{-3}$ and $d = 100\mu$m. Note that in [31] the LiCs sample's OD$\approx$ 500 is rather small, with a lifetime $\sim$ 20 s. The corresponding parameters ($n = 40 \to 39$) for rubidium Rydberg atoms from [30] are also listed for comparison. All data are from [34] (and references therein) except for those otherwise specified.

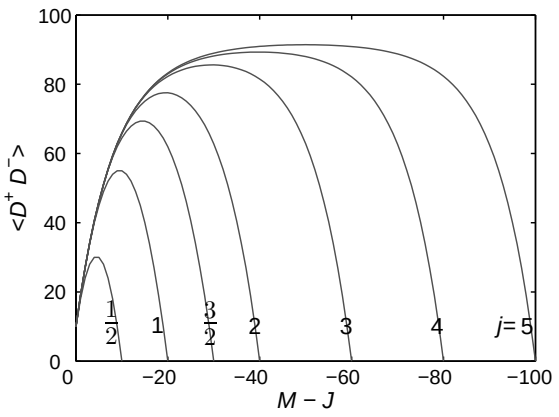

Figure 1: The enhancement factor $\langle D^+D^-\rangle$ versus $M - J$ in the Dicke picture. Note that the left- (right-) hand side corresponds to upper (lower) levels. Different curves correspond to different spin-j cases. Here we have $N = 10$ and $J = Nj$.

considered. We are then able to conclude that the same cooperativity which leads to superradiance for a higher OD still plays an important role here.

This paper is organized as follows: Sec. II discusses the vibrational transitions in the Dicke-superradiance point of view, addressing on the multilevel contribution. Various molecules are also compared according to their vibration relevant parameters in order for better demonstration of superradiance. Sec. III gives the effective master equation based on a mean-field approach, where the two-body coherence is explicitly kept. Then we show our calculation results in Sec. IV, where we also make a comparison for the measured data with our theoretical prediction, taking into account the photon and particle losses as well as the thermal contribution due to blackbody radiation. Finally, Sec. V summarizes this work and future outlook.

II. VIBRATIONAL TRANSITIONS IN THE DICKE LIMIT

In order to see to what degree the superradiance effect must be considered, here we first discuss the optical depth (OD) for different setup of molecules. As it is expected that a larger OD makes superradiance more obvious, a closer vibrational spacing is wanted and hence a larger wavelength. Therefore those molecules with heavier reduced mass become better candidates. On the other hand, the life time from v to $v-1$ transition is usually very long. A larger decay rate γ is preferred so that the transition can be observed before other processes such as chemical reaction destroy the state. For this reason, a stronger dipole moment is preferred. Table I summarizes the relevant parameters for different molecules which are common for cold molecule experiments. Typically the total number of molecules is about a few thousands, being confined within a trap with a diameter $d \approx 10 \sim 100\mu$m. We also lists the values of OD corresponding to currently realizable experiments, showing that quite a range of different molecules should be expected to have superradiance. (From this table, one can see that LiCs is not a good examplifying system because of its light weight and relatively poor OD while KCs and RbCs are best candidates.)

Vibrational states form a multilevel ladder where the low-lying levels are approximately harmonic. Approaching the continuum threshold, the level spacing is getting narrower when the potential curve becomes more anharmonic. For a typical molecule like LiCs, the number of quasi-harmonic vibrational levels can be up to a few tens near the potential minimum. In experiments where the molecules only have a few vibrational excitations, this uniform portion of the vibration ladder should be the main stage where spectroscopy is performed. That is, most of the vibrational transitions are (nearly) degenerate. In such a situation we are urged to consider multilevel effects because the virtual photon exchange, which is the main mechanism to build up the Dicke coherence, can now take place correlating different levels.

In order to see the multilevel effect we reexamine the enhancement factor $\langle JM|D^+D^-|JM\rangle$ in the Dicke picture. Note that in a multilevel case the molecule can be described as a spin-j particle. Therefore $J = Nj$; $-J \le M \le J$; $D^+ \equiv \sum_i D_i^+$ with ith particle $D_i^+ \equiv \sum_{m=-j}^{j-1} |m+1\rangle_i\langle m|$. The generalized Dicke states for spin-j is given by

$$|J, M\rangle = \sqrt{\frac{(J+M)!}{(2J)!(J-M)!}}(\hat{J}^-)^{J-M}|J, J\rangle, \qquad (1)$$

where $\hat{J}^- \equiv \sum_i \hat{j}_i^-$, which satisfy

$$\begin{aligned}\hat{J}^{\pm}|J,M\rangle &= \sqrt{J(J+1)-M(M\pm1)}|J,M\pm1\rangle \\ \hat{j}_i^{\pm}|j,m\rangle &= \sqrt{j(j+1)-m(m\pm1)}|j,m\pm1\rangle_i\end{aligned} \tag{2}$$

with m indexing the single particle vibrational level. Further calculation yields [27, 28] the enhancement factor $\langle D^+D^-\rangle_{JM} = N\langle D_i^+D_i^-\rangle + N(N-1)\langle D_i^+D_j^-\rangle$ with

$$\langle D_i^+D_i^-\rangle = 1 - \langle j, J-j; -j, M+j|J,M\rangle^2 \tag{3}$$

and

$$\begin{aligned}\langle D_i^+D_j^-\rangle = \sum_{m_1,m_2} \Big[&\langle j, J-j; m_1, M-m_1|J,M\rangle \\ &\times \langle j, J-2j; m_2, M-m_1-m_2|J-j, M-m_1\rangle \\ &\times \langle j, J-j; m_1-1, M-m_1+1|J,M\rangle \\ &\times \langle j, J-2j; m_2+1, M-m_1-m_2|J-j, M-m_1+1\rangle\Big].\end{aligned} \tag{4}$$

Figure 1 plots the enhancement factor $\langle D^+D^-\rangle_{JM}$ as a function of $M-J$ for various spin-j particles. It is shown that the decay rate increases in general as the number of levels increases. At $M \approx J$, all the curves coincide, indicating that they share the same emission behavior while starting emitting. The enhancement continues to grow as M lowers before it peaks around $M \approx 0$; then it turns to decrease with descending M and finally vanishes at $M = -J$. It is worth noting that the curve forms a plateau for large j around a range of middle M, and most importantly the ascending part of the curve keeps invariant as j increases. This suggests that the exact number of levels is not important in determining the initial emission behavior as long as the number of levels is large enough. This is valid in typical vibrational spectroscopy within a small timescale (compared to γ^{-1}).

III. TWO-BODY MASTER EQUATION

The previous approach concerning Dicke superradiance in the multilevel case does not take into account the finite spatial size of the sample and other decoherence mechanism such as dephasing. These additional factors can be contained by considering explicitly the actual dipole-dipole interaction. On one hand, dipole-dipole interaction induced spin (two-level particle) flip-flop, or the so-called virtual photon exchange, is the major mechanism for generating and maintaining the Dicke type of coherence. On the other hand, the dipole-dipole interaction ($\sim r^{-3}$, where r is the inter-particle distance) also introduces dephasing that suppresses superradiance. These effects can be contained in the microscopic Hamiltonian [28]:

$$H = \underbrace{H_{\text{atom}} + H_{\text{field}} - \sum_{i\notin\{1,2\}} \mathbf{p}_i\cdot\mathbf{E}_i(t)}_{H_0} \underbrace{-\sum_{i=1}^{2}\mathbf{p}_i\cdot\mathbf{E}_i(t)}_{V}), \tag{5}$$

where V represents two probe particles ($i = 1, 2$) interacting with the local field due to environmental particles as well as the external field, whose degrees of freedom have been absorbed in H_0. In this approach, V is considered to be a perturbative term with respect to H_0. Our goal is to derive an effective description for the two probe atoms in a mean-field manner, which can be thought as the next order correction beyond the single particle mean-field approximation. Our strategy is to integrate out irrelevant degrees of freedom such as field variables and environmental dipoles by means of the Schwinger-Keldysh Green's function approach. Here a Gaussian field is assumed so that we are allowed to only keep up to the second order of field correlation. Then the induced rate is determined by the field-field correlation. The detail of derivation can be found in [27, 28] and we arrive at the effective master equation:

$$\begin{aligned}\dot{\rho} = &-\frac{\Gamma}{2}\sum_{i=1}^{2}\left(\rho D_i^-D_i^+ + D_i^-D_i^+\rho - 2D_i^+\rho D_i^-\right) \\ &-\frac{\Gamma+\gamma}{2}\sum_{i=1}^{2}\left(\rho D_i^+D_i^- + D_i^+D_i^-\rho - 2D_i^-\rho D_i^+\right) \\ &-\bar{\Gamma}\sum_{i\neq j}\left(\rho D_i^-D_j^+ + D_i^-D_j^+\rho - 2D_j^+\rho D_i^-\right),\end{aligned} \tag{6}$$

where ρ is the two-body density matrix whose dimension is $(2j+1)\times(2j+1)$, and

$$\Gamma = \gamma(e^{2\zeta}-1)\frac{A(t)}{V(t)} + 2\mathcal{C}^2\varrho^4\frac{\gamma^2 I(\zeta,\varrho)}{\Gamma+\gamma/2}Y(t) \tag{7}$$

$$\bar{\Gamma} = \frac{\gamma^2 I(\zeta,\varrho)}{\Gamma+\gamma/2}\left[3\mathcal{C}\varrho A(t) + 2\mathcal{C}^2\varrho^4 Y(t)\right] \tag{8}$$

with

$$\begin{aligned}A(t) &= \sum_{m=-j+1}^{j}\rho_{mm}^{(1)} \\ V(t) &= \rho_{jj}^{(1)} - \rho_{-j,-j}^{(1)} \\ Y(t) &= \sum_{m,m'=-j}^{j-1}\rho_{m+1,m;m',m'+1}.\end{aligned} \tag{9}$$

Here $\rho^{(1)} \equiv \frac{1}{2}\sum_{i=1,2}\mathrm{tr}_i[\rho]$ denotes the reduced single-particle density matrix and $\rho_{ab;cd} \equiv \frac{1}{2}[\langle a,c|\rho|b,d\rangle + \langle c,a|\rho|d,b\rangle]$, where by $|a,c\rangle$ we denote $|a\rangle_1\otimes|c\rangle_2$. For both the factor $\frac{1}{2}$ comes from averaging the interchanging of two particles. Note that interchange symmetry requires $\rho_{ab;cd} = \rho_{cd,ab}$ and $\rho^*_{ab;cd} = \rho_{ba;dc}$. The cooperativity parameter is defined as $\mathcal{C} \equiv 2\pi\mathcal{N}c^3/\omega_0^3$ with the particle density $\mathcal{N}$; $\varrho \equiv \omega_0 d/(2c)$ characterizes the system size d in units of the radiation wavelength. Function $I(\zeta,\varrho) \equiv e^{2\zeta}[(\zeta-1)^2+\varrho^2]/(\zeta^2+\varrho^2)^2$. With these definitions, $\mathrm{OD} = 4\pi\mathcal{C}\varrho$.

Each term of master equation (6) can be understood as follows: The first line accounts for population pumping

with the induced rate Γ. The opposite process, i.e., decay, is also characterized by Γ, as presented in the second line. In addition, the free-space spontaneous decay with a rate γ takes place and is contained in the second line. Note that at a finite temperature, the thermal contribution of blackbody radiation may cause extra incoherent pumping and decay. This effect can be introduced by adding an additional rate $B \approx \gamma/(e^{\beta\hbar\omega_0} - 1)$ with $\beta^{-1} = k_B T$ [31] to Γ. Further, the population pumping corresponds to photon re-absorption (real photons only, not virtual photons). This, however, may depends on the scattering rate of photons and particles. In order to characterize the efficiency of re-absorption, we replace in the first line $\Gamma \longrightarrow s\Gamma$, where the factor $s = 1$ corresponds to maximal re-absorption of emitted photons and $s = 0$ represents loss of emitted photons entirely. Although at this point we do not estimate s quantitatively, these two extremes $s = 0, 1$ should be able to give the lower and upper bounds for the actual behavior. The third line corresponds to generation and reduction of inter-particle coherence with a rate $\bar{\Gamma}$. Finally, considering the current experimental setup, where there is inevitably particle loss out of the trap, one more term $-\gamma_L \rho$ must be added into to master equation (6). Note that this term does not preserve unity trace of the density matrix as time evolves.

IV. RESULTS AND DISCUSSION

A. Multilevel enhancement

We have investigated the multilevel superradiance in great detail in [27]. For completeness, here we include a brief discussion for this effect. Such an enhancement is due to the fact that the cross-level virtual photon exchange is more possible. In a two-level system, when a particle emits a real photon but fails to keep correlation to other particles due to certain dephasing, it no longer participates in the superradiance coherence unless it gets excited later and re-enters the game. This is different in the multilevel case because a highly excited particle can be involved in manybody correlation for several times of its transitions before the ground state is reached. Fig. 2 (a) shows the emission intensity $I_{\rm em}$ as a function of time, where $I_{\rm em} \equiv \hbar\omega_0 \frac{d}{dt} \sum_v v\rho_{vv}^{(1)}$ corresponding to the overall outgoing radiated energy per unit time. These curves are dramatically different from an exponential profile yielded by single atoms. The initial increase and hump in the intensity is the signature for superradiance. Note that the rising parts of the curves coincide for various level numbers, except that a larger discrepancy is observed in the two-level case. This coincidence even extends for longer times in the many level cases; the hump is bounded in the limit of large level numbers. This can be understood by looking at Fig. 2 (b), where we show the top five levels' population distribution (diagonal terms of the reduced single particle density matrix) over the vibrational ladder at the time when the intensity value is peaked.

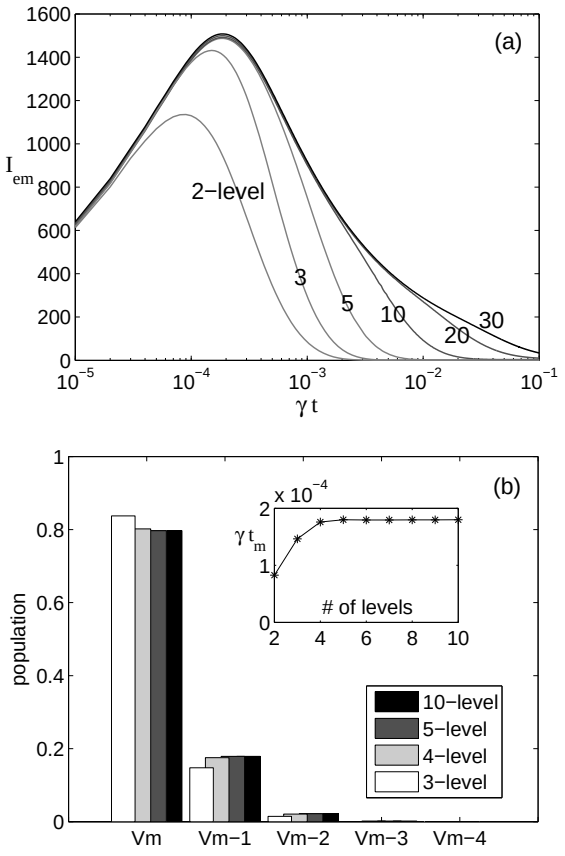

Figure 2: (a) Emission intensity as a function of time. Different curves correspond to different number of vibrational levels. For all data, OD $= 3.8 \times 10^4$. (b) Population distribution of the five highest levels for 3, 4, 5, and 10-level cases at peak intensity (when $t = t_m$). V_m denotes the highest level where the whole system is initially populated. Inset: γt_m as a function of the number of levels.

We can see that the distribution is almost identical for various cases. This happens because the initial emission behavior is determined only by the nearby levels. Those levels far below do not contribute.

B. Comparison with experiment

In usual cold molecule experiments, individual atoms are first loaded and cooled in a trap and then through photoassociation Feshbach molecules can be formed. In most situations, the electronic state of the molecules is kept on the ground state but not for vibrational and rotational states. In a recent experiment done by Deiglmayr *et al.,* the vibrational population redistribution of LiCs molecules was investigated [31]. An unusual discrepancy was found between the experimental data and the simulated curves given by rate equation approaches based on Einstein's A-coefficients and inclusion of blackbody radiation. Here we apply the superradiance formalism

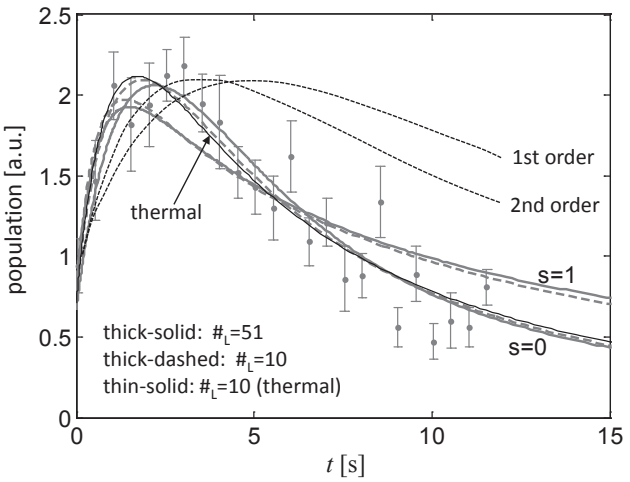

Figure 3: Fitting curves by adjusting the ratio N_4/N_3 between the population of levels $v = 3$ and $v = 4$. For $s = 1$, i.e., the re-absorption is considered, the optimized ratio $N_4/N_3 = 7.47$; for $s = 0$, i.e. the re-absorption is neglected, the ratio $N_4/N_3 = 6.72$. An optimization is also taken by overall rescaling the y value for best fit. For comparison, two simulated curves from [31] are plotted, corresponding to inclusion of the first-order and second-order particle losses, respectively. The thin-solid line corresponds to the case when the balckbody radiation is considered, with the optimized ratio $N_4/N_3 = 7.55$. The resultant difference, however, is rather small. The scattered dots with error bars are the experimental data.

to their experimental setup, where OD ≈ 500. In Fig. 3 we show the time evolution of the population profile corresponding to level $v = 3$, directly comparable to the photoassociation measurement outcome.

We fit the experimental data as follows: From [31] we find the ratios of the lowest ten vibrational levels. In the experiment, however, most electrons ($\sim$70%) are still in some of the upper levels, with unknown distribution. Thus, we have to allow for at least one fitting parameter to take this unknown into account. In our case, for ease of calculation, this fitting parameter is the ratio between the population of levels $v = 3$ and $v = 4$. The curves are then calculated for 51 total levels and an approximation where only the lowest 10 of those 51 levels are used (Fig. 3 shows that there is nearly no difference between those two cases.)

In Fig. 3, the scattered dots with error bars represent the experimental data and the thick-solid (thick-dashed) lines correspond to the overall 51-level (10-level truncated) case. For comparison, we plot $s = 0$ and $s = 1$ cases corresponding to the upper and lower bounds, respectively, when re-absorption efficiency is 0 or maximized. We find that the $s = 0$ curves show a very good agreement with the experimental data, suggesting that re-absorption is not a significant effect when the trap is transparent to radiation. Most importantly, such agreement implies that superradiance (or at least the inter-particle cooperativity) plays an important role in determining the relaxation behavior. It is notable that, in this experiment, OD ≈ 500 is very low, even lower than the values suggested in Table I. It is actually near the boundary of superradiance and ASE. Note that ASE as well as superradiance are both caused by the dipole-dipole interaction. But in ASE the decoherence dominates and therefore the inter-particle coherence is less pronounced. It should be emphasized that the ASE mechanism is also contained under the framework of our approach. In fact, LiCs is a rather bad choice for demonstrating superradiance because of its low reduced mass. A heavier species such as RbCs under similar experimental setup will do better (see Table I).

C. Blackbody radiation

An additional curve (thin-solid line) is also plotted in Fig. 3, taking into account the thermal contribution of blackbody radiation. But the deviation is rather small. Here we briefly discuss the role of the blackbody radiation repumping and decay. In Eq. (6) it serves as a factor in addition to Γ. At room temperature $T = 300$K, we can estimate $B = 0.75\gamma$. This is usually a significant quantity in the single particle case but not in the superradiance case, where Γ is typically 2 orders of magnitude larger than γ for OD $= 10^2 \sim 10^3$.

V. CONCLUSION

The vibrational relaxation behavior of cold molecules displays superradiant behavior when their density is large so their particle cooperativity must be considered. We have developed a mean-field method that explicitly take into account the actual dipole contribution as well as the multilevel effect. Our theory works rather well describing the experimental data from measuring the relaxation of vibrational population for cold molecules. This indicates that the cooperativity has a significant effect regarding spectroscopy in most ultracold molecules experiments, including vibrational and/or rotational transitions. Our calculations suggest that considerable cooperative effects can be expected from a large amount of ultracold molecule experiments if vibrational and rotational transitions are considered. In general, for all setups with an OD density of the order of $10^2 \sim 10^3$ or higher, superradiance will play an important role.

Some open questions remain such as how superradiance is modified by (1) the anharmonicity of the vibrational ladder, (2) the non-constant transition dipole moments from level to level, and (3) the trap-induced inhomogeneity in density. They are, however, at this point not expected to have a major qualitative impact on the results.

Acknowledgments

We would like to thank NSF and AFOSR for funding, and M. Repp, J. Deiglmayr, and M. Weidemüller for discussions.

[1] V. V. Flambaum, Phys. Rev. A **73**, 034101 (2006).
[2] V. V. Flambaum and M.G. Kozlov, Phys. Rev. Lett. **99**, 150801 (2007).
[3] J. J. Hudson, B. E. Sauer, M. R. Tarbutt and E. A. Hinds, Phys. Rev. Lett. **89**, 023003 (2002).
[4] M. S. Malcuit, J. J. Maki, D. J. Simkin and R. W. Boyd, Phys. Rev. Lett. **59**, 1189 (1987).
[5] E. L. Bolda, R. Y. Chiao and J. C. Garrison, Phys. Rev. A **52**, 3308 (1995).
[6] R. H. Dicke, Phys. Rev. **93**, 99 (1954).
[7] F. T. Arecchi and E. Courtens, Phys. Rev. A **2**, 1730 (1970).
[8] R. H. Lehmberg, Phys. Rev. A **2**, 883 (1970).
[9] N. E. Rehler and J. H. Eberly, Phys. Rev. A **3**, 1735 (1971).
[10] C. R. Stroud, J. H. Eberly, W. L. Lama and L. Mandel, Phys. Rev. A **5**, 1094 (1972).
[11] R. Friedberg and S. R. Hartmann, Phys. Rev. A **10**, 1728 (1974).
[12] R. Bonifacio and L. A. Lugiato, Phys. Rev. A **11**, 1507 (1975).
[13] M. Gross and S. Haroche, Physics Reports **93** (5), 301 (1982).
[14] G. Feher, J. P. Gordon, E. Buehler, E. A. Gere and C. D. Thurmond, Phys. Rev. **109**, 221 (1958).
[15] N. Skribanowitz, I. P. Herman, J. C. MacGillivray and M. S. Feld, Phys. Rev. Lett. **30**, 309 (1973).
[16] Q. H. F. Vrehen, H. M. J. Hikspoors and H. M. Gibbs, Phys. Rev. Lett. **38**, 764 (1977).
[17] F. Gounand, M. Hugon, P. R. Fournier and J. Berlande, Journal of Physics B: Atomic and Molecular Physics **12** (4), 547 (1979).
[18] J. M. Raimond, P. Goy, M. Gross, C. Fabre and S. Haroche, Phys. Rev. Lett. **49**, 1924 (1982).
[19] P. Goy, J. M. Raimond, M. Gross and S. Haroche, Phys. Rev. Lett. **50**, 1903 (1983).
[20] L. Moi, P. Goy, M. Gross, J. M. Raimond, C. Fabre and S. Haroche, Phys. Rev. A **27**, 2043 (1983).
[21] S. Inouye, A. P. Chikkatur, D. M. Stamper-Kurn, J. Stenger, D. E. Pritchard and W. Ketterle, Science **285** (5427), 571 (1999).
[22] M. Scheibner, T. Schmidt, L. Worschech, A. Forchel, G. Bacher, T. Passow and D. Hommel, Nat Phys **3** (2), 106 (2007).
[23] J. G. Bohnet, Z. Chen, J.M. Weiner, D. Meiser, M. J. Holland and J. K. Thompson, Nature **484** (7392), 78 (2012).
[24] J. C. MacGillivray and M. S. Feld, Phys. Rev. A **14**, 1169 (1976).
[25] J.-H. Chen and X.-A. Mao, Journal of Physics D: Applied Physics **32** (7), 764 (1999).
[26] E. Akkermans, A. Gero and R. Kaiser, Phys. Rev. Lett. **101**, 103602 (2008).
[27] G.-D. Lin and S. F. Yelin, Phys. Rev. A **85**, 033831 (2012).
[28] G.-D. Lin and S. F. Yelin, Superradiance: An Integrated Approach to Cooperative Effects in Various Systems, in *Advances in Atomic, Molecular, and Optical Physics*, edited by Ennio Arimondo, Paul Berman, and Chun Lin, Vol. 61, Chap. 6 (2012), pp. 295 – 329.
[29] S. M. Farooqi, D. Tong, S. Krishnan, J. Stanojevic, Y. P. Zhang, J. R. Ensher, A. S. Estrin, C. Boisseau, R. Côt E. E. Eyler and P. L. Gould, Phys. Rev. Lett. **91**, 183002 (2003).
[30] T. Wang, S. F. Yelin, R. Côt E. E. Eyler, S. M. Farooqi, P. L. Gould, M. Koštrun, D. Tong and D. Vrinceanu, Phys. Rev. A **75** (3), 033802 (2007).
[31] J. Deiglmayr, M. Repp, O. Dulieu, R. Wester and M. Weidemüller, Eur. Phys. J. D **65** (1-2), 99 (2011).
[32] M. Aymar and O. Dulieu, The Journal of Chemical Physics **122** (20), 204302 (2005).
[33] K. K. Ni, S. Ospelkaus, M. H. G. de Miranda, A. Pe'er, B. Neyenhuis, J. J. Zirbel, S. Kotochigova, P. S. Julienne, D. S. Jin and J. Ye, Science **322** (5899), 231 (2008).
[34] National Institute of Standards and Technology, NIST Chemistry WebBook, *http://webbook.nist.gov/chemistry.*